Biochimica et Biophysica Acta 1837 (2014) 1257–1262

Contents lists available at ScienceDirect

Biochimica et Biophysica Acta

journal homepage: www.elsevier.com/locate/bbabio

# Substrate water exchange in photosystem II core complexes of the extremophilic red alga *Cyanidioschyzon merolae*☆

Håkan Nilsson [a], Tomasz Krupnik [b], Joanna Kargul [b], Johannes Messinger [a,*]

[a] Department of Chemistry, Kemiskt Biologiskt Centrum (KBC), Umeå University, S-901 87 Umeå, Sweden
[b] Department of Plant Molecular Physiology, Faculty of Biology, University of Warsaw, Miecznikowa 1, 02-096 Warsaw, Poland

ARTICLE INFO

*Article history:*
Received 22 February 2014
Received in revised form 31 March 2014
Accepted 1 April 2014
Available online 12 April 2014

*Keywords:*
*Cyanidioschyzon merolae*
Photosystem II
Water oxidation
Oxygen evolution
Substrate–water exchange
Membrane-inlet mass spectrometry

ABSTRACT

The binding affinity of the two substrate–water molecules to the water-oxidizing $Mn_4CaO_5$ catalyst in photosystem II core complexes of the extremophilic red alga *Cyanidioschyzon merolae* was studied in the $S_2$ and $S_3$ states by the exchange of bound $^{16}O$-substrate against $^{18}O$-labeled water. The rate of this exchange was detected *via* the membrane-inlet mass spectrometric analysis of flash-induced oxygen evolution. For both redox states a fast and slow phase of water-exchange was resolved at the mixed labeled *m/z* 34 mass peak: $k_f = 52 \pm 8\ s^{-1}$ and $k_s = 1.9 \pm 0.3\ s^{-1}$ in the $S_2$ state, and $k_f = 42 \pm 2\ s^{-1}$ and $k_{slow} = 1.2 \pm 0.3\ s^{-1}$ in $S_3$, respectively. Overall these exchange rates are similar to those observed previously with preparations of other organisms. The most remarkable finding is a significantly slower exchange at the fast substrate–water site in the $S_2$ state, which confirms beyond doubt that both substrate–water molecules are already bound in the $S_2$ state. This leads to a very small change of the affinity for both the fast and the slowly exchanging substrates during the $S_2 \rightarrow S_3$ transition. Implications for recent models for water-oxidation are briefly discussed.



## 1. Introduction

The molecular oxygen we breathe is produced by cyanobacteria, algae and higher plants *via* light-induced water oxidation in photosystem II (PSII). This reaction occurs within the oxygen evolving complex (OEC) that catalyzes the oxidation of two water molecules into molecular oxygen, four protons and four electrons. This complex is comprised of four manganese atoms and one calcium atom, which are connected by five μ-oxo bridges. These atoms are arranged in a chair-like structure with a distorted cubane base ($Mn_4CaO_5$ cluster) [1–6]. Four consecutive flashes lead *via* sequential charge separations in the chlorophyll-containing reaction center of PSII to the accumulation of four oxidizing equivalents in the OEC, which subsequently liberates $O_2$. To describe this reaction cycle, which was deduced from flash-induced oxygen evolution patterns [7], Kok and coworkers introduced the S state model, also known as the Kok cycle, with five different oxidation states of the OEC [8]. The S state model denotes the number of stored oxidizing equivalents in a particular S state by the index *i* ($S_i$: $S_0$–$S_4$). The molecular mechanism captured by this elegant kinetic scheme is presently not fully understood and different mechanisms have been proposed [3,9–16].

*Cyanidioschyzon merolae* is an extremophilic red microalga that naturally grows at extremely low pH (pH 0.2–4) and moderately high temperatures (40–56 °C) [17,18]. The composition of the extrinsic lumenal proteins of PSII stabilizing the OEC differs somewhat from that of higher plants, green algae and prokaryotic cyanobacteria [19]. Higher plants and green algae both contain PsbO, PsbP, and PsbQ (and possibly PsbR), whereas red algae contain PsbO, PsbP, PsbQ' (CyanoQ homologue), PsbU and PsbV. Cyanobacteria contain PsbO, PsbU, PsbV and the cyanobacterial homologues of PsbP and PsbQ: CyanoP and CyanoQ. Notable is the intermediate composition of extrinsic proteins in red algae compared to prokaryotes and eukaryotes. A 17 Å electron density map derived from electron microscopy and single particle analysis of the *C. merolae* dimeric PSII particles has recently been published together with a functional study of this complex under extreme conditions [20]. In the same study it was found that *C. merolae* PSII retained significant photosynthetic activity in an unusually broad range of pH, temperatures and light intensities. Since the mechanism of water-oxidation is known to be highly dependent on the prompt release of

*Abbreviations:* *C. merolae*, *Cyanidioschyzon merolae*; PSII, photosystem II; PSIIcc, photosystem II core complexes; OEC, oxygen evolving complex; S states ($S_i$), oxidation states of the OEC; $W_f$, fast exchanging substrate–water; $W_s$, slowly exchanging substrate–water; $k_s$, rate constant of slow water exchange; $k_f$, rate constant of fast water exchange; TR-MIMS, time resolved membrane inlet mass spectrometry; FIOPs, flash induced oxygen evolution pattern

☆ This paper is dedicated to the memory of Warwick Hillier (18.10.1967–10.01.2014). Using membrane-inlet mass spectrometry and FTIR spectroscopy Warwick made many important discoveries regarding substrate–water binding to the OEC and the mechanism of water-oxidation. He was a very good scientist and friend who was highly appreciated throughout the photosynthesis community. In 2007 he was awarded the Robin-Hill Award of the International Society for Photosynthesis Research (ISPR).

* Corresponding author at: Department of Chemistry, Chemical Biological Centre (KBC), Umeå University, 901 87 Umeå, Sweden.
*E-mail address:* Johannes.Messinger@umu.se (J. Messinger).

http://dx.doi.org/10.1016/j.bbabio.2014.04.001

protons produced during water-oxidation [21], it is highly interesting to study if this greater pH stability of PSII is related only to the above-described differences in the protein composition, or if the kinetic parameters of the OEC may also be changed, such as the binding affinity of the $Mn_4CaO_5$ catalyst for the two substrate–water molecules.

The time resolved membrane inlet mass spectrometry (TR-MIMS) approach used in this study gives information on how the affinity of the manganese catalyst for water substrate changes during the S state transitions [22]. The affinity can be directly probed by exchanging already bound $H_n^{16}O$ substrates (n = 0, 1, 2) with bulk $H_2^{18}O$. This exchange can be then probed by photo-generating oxygen release after various incubation times followed by the analysis of the isotopic composition of thus produced $O_2$ by isotope ratio mass spectrometry [13, 22–30]. Here, we present for the first time substrate–water exchange rates in the highly stable dimeric PSII core complexes isolated from the extremophilic red alga *C. merolae* [17]. We discuss the mechanistic implications of these data in the context of the substrate–water exchange rates obtained previously for the purified spinach and cyanobacterial PSII core complexes [23,25].

## 2. Materials and methods

### 2.1. Purification of C. merolae PSII dimers

Cell culturing, isolation of thylakoids and purification of dimeric PSII particles were performed essentially as described in [20]. Following solubilization of thylakoids (1 mg/mL Chl*a*) with 1% (w/v) dodecyl-β-D-maltoside, dimeric PSII core complexes were purified by anion exchange chromatography on DEAE Toyopearl 650M and DEAE Toyopearl 650S media, using a continuous NaCl gradient (0.05–0.15 M NaCl), as described in detail in [20]. The purity of dimeric PSII core complexes (PSIIcc) was assessed by SDS-PAGE, size exclusion chromatography (SEC) and spectrophotometrically, according to the procedures described in [20].

### 2.2. PSII activity measurement

The oxygen evolving activity of purified dimeric PSIIcc was measured using a Clark-type oxygen electrode (Hansatech). Measurements were performed at 30 °C in a buffer composed of 40 mM MES-KOH pH 6.1, 10 mM $CaCl_2$, 5 mM $MgCl_2$, 25% (w/v) glycerol in the presence of 0.125 mM 2,6-dichloro-*p*-benzoquinone (Sigma, Germany) and 2.5 mM potassium ferricyanide (POCH, Poland) as the exogenous electron acceptors. Samples (1 μg/mL Chl) were illuminated with a white light intensity of 5000 μE/$m^2$/s, using a KL 2500 LCD white light source (Schott, Germany). Activities were calculated from initial rates of oxygen evolution curves. Each measurement was repeated 3 times. The average activity of dimeric PSII was 4500 μmol $O_2$/mg Chl/h, and was consistent across multiple preparations.

### 2.3. Membrane-inlet mass spectrometry

An isotope ratio mass spectrometer (ThermoFinnigan Delta plus XP) connected to a membrane inlet sample chamber (165 μL) *via* a cooling trap (dry ice) was used for the time-resolved membrane inlet mass spectrometry measurements (TR-MIMS) described in this study. TR-MIMS measurements were performed at *m/z* 32, *m/z* 34 and *m/z* 36 to quantify the flash-induced oxygen production from PSII samples as described previously [22,31]. The samples were stored at −80 °C. Prior to measurements, the sample aliquots were thawed on ice and diluted in measuring buffer (pH 6.1, 10 mM $CaCl_2$, 5 mM $MgCl_2$, 40 mM Mes, 1 M betaine) to a chlorophyll concentration of 0.3 mg/mL. Synchronization in the $S_1Y_D^{ox}$ state was achieved by pre-flashing each sample aliquot (300 μL, Chl [0.3 mg/mL]) once with a Xenon flash lamp (~5 μs FWHM), followed by dark adaptation for 1 h at 20 °C. After 40 min dark-adaptation the sample aliquot (165 μL) was loaded into the membrane inlet sample chamber. After 20 min of degasification under continuous stirring at 20 °C, the sample was advanced to the $S_2$ state with one flash (or two flashes at 2 Hz to attain the $S_3$ state) (~6 μs FWHM). Rapid injection ($t_{1/2}$ = 3 ms) of $H_2^{18}O$ (97.7%) with a gas tight syringe (Hamilton CR-700-50) into the cuvette enriched the sample with $H_2^{18}O$ (24% final). The dissolved oxygen in the $H_2^{18}O$ aliquot was removed prior to injection by adding glucose, glucose oxidase and catalase. The rapid $H_2^{18}O$ injection was initiated with a computer (LabView software), which triggered the release of 8 bars $N_2$ from a fast switching valve (FESTO MHE2-MS1H 3/2G-M7-K) that pushed a pneumatic piston (Festo AEVC-12-10-A-P) connected to the syringe plunger [22]. The same computer also controlled the timing of the subsequent flashes that initiate the $O_2$ release after defined incubation times. The time for subtrate-water exchange was varied between 0 s and 10 s by injecting $H_2^{18}O$ at various time points before giving two turnover flashes at 100 Hz ($S_2$ state exchange) or one turnover flash ($S_3$ state). The oxygen yields of the substrate–water exchange measurements were corrected for flash-induced double hits and injection artifacts as described in [22,23], and normalized by giving 4 flashes at 2 Hz 5 min after the third turnover flash. At very short incubation/exchange times corrections were also made to account for the isotopic enrichment and chlorophyll concentration present in the sample at the time of illumination [23].

### 2.4. Rate of $H_2^{18}O$ injection and mixing

The rate of $H_2^{18}O$ injection into the cuvette and the time for complete mixing with a sample was determined in separate experiments by measuring fluorescence as a function of time after fluorescein injection. The fluorescein solution (30 μM, 40 μL) was injected into the cuvette prefilled with a buffer solution (0.1 M Tris pH 8.0, 165 μL). The fluorescein was excited by a LED lamp (Luxeon V-Star blue, 1 W) *via* a band pass filter (Newport 470 nm–495 nm) and fiber optic tube. The resulting fluorescence (fluorescein — $\lambda_{ex}$ 490 nm; $\lambda_{em}$ 525 nm) was guided *via* a bifurcated optical fiber and a second band pass filter (Newport 520 nm–547 nm). A photodiode (Hamamatsu S-2281/C9329) converted the fluorescence into an electrical signal that was measured with an oscilloscope.

### 2.5. Flash-induced oxygen-evolution pattern

The flash-induced oxygen-evolution pattern (FIOP) was obtained using TR-MIMS by giving 16 flashes separated by dark times of 25 s (Xenon flash lamp, ~5 μs FWHM). The experiments were performed at 20 °C and pH 6.1 ($CaCl_2$ 10 mM, $MgCl_2$ 5 mM, Mes 40 mM, betaine 1 M) at a chlorophyll concentration of 0.33 mg Chl/mL. Prior to loading into the MIMS cell, the sample was pre-flashed once and mixed with $H_2^{18}O$ (10% v/v), followed by dark adaptation for 1 h at 20 °C. An Excel spreadsheet program that was based on the extended Kok model was used to fit the FIOP.

## 3. Results

### 3.1. Flash-induced oxygen pattern (FIOP)

Fig. 1 shows the flash induced oxygen yield pattern (FIOP) of the *C. merolae* dimeric PSII core particles that was obtained at *m/z* 34 in the absence of artificial electron acceptors. The $O_2$ oscillation pattern shows the characteristic features of the Kok model, with a maximum of oxygen yield after the third flash. As typical for core preparations, only a very small second oscillation is observed due to the limited plastoquinone pool. The oscillation can be fit with a miss parameter $\alpha = 19$, a double hit parameter $\beta = 4$, and 100% $S_1$ state population in the dark-adapted sample [8,32]. The slightly high miss parameter is likely due to the long dark-times of 25 s that are required for resolving the oxygen yields after each flash individually.

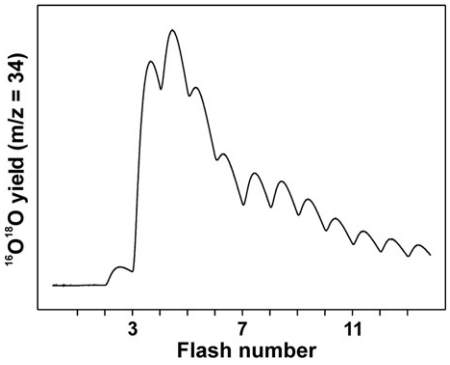


**Fig. 1.** Flash-induced oxygen evolution pattern (FIOP) of *C. merolae* PSIIcc. Evolution of $^{16}O^{18}O$ was induced by 16 saturating Xe-flashes and detected by membrane-inlet mass spectrometry. The dark-times between flashes were 25 s. Other parameters: 20 °C, pH 6.1, 10% (v/v) $H_2^{18}O$.

### 3.2. Substrate–water exchange rates

This good oscillation allows for the determination of the substrate–water exchange rates *via* time-resolved isotope-labeling MIMS. Fig. 2 shows the rise of the *m/z* 34 and *m/z* 36 signals as a function of substrate–water exchange time at 20 °C and pH 6.1. The fast phase of the characteristic biphasic rise of the *m/z* 34 signal is attributed to the exchange of the fast exchanging $H_2O$ ($W_f$), whereas the slower phase represents the slowly exchanging substrate–water ($W_s$) [22]. Notably, the fast exchange in the $S_2$ state is very well resolved compared to all earlier studies with PSII from other organisms. At *m/z* 36 the exchange of $W_s$ is rate limiting and thus only a mono exponential rise is observed [22,23].

**Table 1**
Substrate–water $H_2^{18}O/H_2^{16}O$ exchange rate constants for *C. merolae* PSIIcc. $H_2^{18}O/H_2^{16}O$ exchange was measured in the $S_2$ and $S_3$ states at 20 °C, pH 6.1. The rates for the fast ($k_f$) and slow ($k_s$) were obtained by fitting the rise of the labeled $^{16,18}O_2$ and $^{18,18}O_2$ oxygen products with $H_2^{18}O$ incubation time (Fig. 1) with Eqs. (1) and (2), respectively.

| S state | $k_f$, $s^{-1}$ | $k_s$, $s^{-1}$ |
|---|---|---|
| $S_3$ | 42 ± 2 | 1.2 ± 0.3 |
| $S_2$ | 52 ± 8 | 1.9 ± 0.3 |

The exchange rates (Table 1) were obtained by fitting (solid line) the data with the sum of two exponential functions for *m/z* 34:

$$^{34}Y = 0.66 \cdot \left(1 - \exp\left(-^{34}k_f \cdot t\right)\right) + 0.34 \cdot \left(1 - \exp\left(-^{34}k_s \cdot t\right)\right) \quad (1)$$

where the pre-exponential factors are dependent on the final $H_2^{18}O$ concentration, as explained in references [22,23].

The time course at *m/z* 36 was fit by the single exponential function:

$$^{36}Y = 1 - \exp\left(-^{36}k \cdot t\right). \quad (2)$$

The values of the slow components measured at *m/z* 34 ($^{34}k_s$) and *m/z* 36 ($^{36}k$) were forced to be identical during the fits, and therefore only $k_f$ and $k_s$ are given in Table 1.

The data in Table 1 show that the substrate–water exchange rates slow down during the $S_2 \rightarrow S_3$ transition by a factor of 1.6 for $W_s$ and 1.2-fold for $W_f$. These findings signify a small increase in the substrate affinity for both $W_s$ and $W_f$ during the $S_2 \rightarrow S_3$ transition.

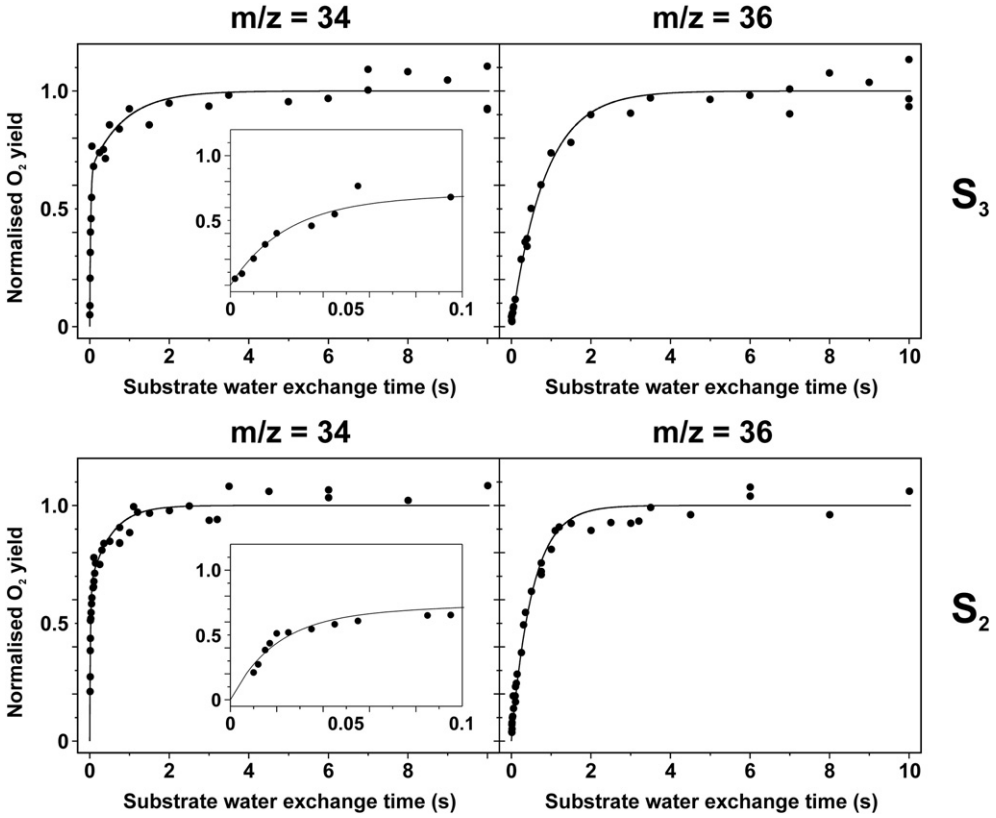


**Fig. 2.** Substrate–water exchange in the $S_3$ (top panels) and $S_2$ (bottom panels) states of *C. merolae* PSIIcc. The normalized $O_2$ yield (symbols) as a function of the time after $H_2^{18}O$ injection (final enrichment, 24%) is plotted. The solid lines are kinetic fits to the biphasic exchange at *m/z* 34 and the monophasic exchange at *m/z* 36 according to Eqs. (1) and (2), respectively. The rate constants to the fits are given in Table 1. The measurements were performed at 20 °C and pH 6.1.

## 4. Discussion

### 4.1. Both substrate–waters are bound in the $S_2$ state

More and more details are presently revealed about the mechanism of photosynthetic water oxidation [33–35]. One important aspect for fully understanding this mechanism is the elucidation of the two substrate–water-binding sites, and how the protonation, oxidation and binding states of the two substrate–waters change during the S state cycle. The slowly exchanging water has been suggested to be an oxo-bridge between Ca and Mn, and specifically the bridge known presently as O5 [15,28,29]. This notion is based on the observed increase in the exchange rate of $W_s$ if Ca is replaced by Sr [28] and the S state dependent differences of its exchange rate [13,15]. Strong support for this possibility came from DFT calculations [36] and, recently, from EPR/ESEEM and $^{17}$O-exchange ELDOR-detected NMR studies at W-band that demonstrated that the oxo-bridge O5 can incorporate the $^{17}$O label from the bulk within 15 s [30,37].

Two different structures of the $Mn_4CaO_5$ cluster have been proposed to be in equilibrium in the $S_2$ state, and it is not clear at this point which structure the cluster attains in the $S_3$ and $S_4$ states [38–41]. The two $S_2$ state structures differ in the position of the central O5 oxo-bridge, which may be either bound between Ca, $Mn_{B3}$ and $Mn_{A4}$ (open cube structure; outer position), or between Ca, $Mn_{B3}$ and $Mn_{D1}$ (closed cube configuration; inner position, see Fig. 3). Depending on which structure is favored for the higher S states, three different binding sites for the fast exchanging water were put forward: $Mn_{A4}$, Ca and $Mn_{D1}$ [15,40,42–44]. Accordingly, W2, W3 or a water molecule (WX) postulated to bind to $Mn_{D1}$ during the $S_2 \rightarrow S_3$ state transition would be in 'striking' distance to O5, the suspected slowly exchanging substrate $W_s$.

It is therefore mechanistically important that in this study the fast substrate–water exchange was clearly resolved in the $S_2$ state, where the structure of the $Mn_4CaO_5$ cluster is relatively well established. Previously, only two other studies detected the fast exchange in $S_2$ [26,27]. In spinach thylakoids the fast exchange in $S_2$ was resolved at 10 °C (120 $s^{-1}$), but not at 20 °C [26]. A similar rate was reported earlier for spinach BBY preps, which were depleted of the extrinsic 16 and 23 kDa protein by salt washing [27]. Since this rate is very close to the time-resolution of the instrumentation, which is determined by the speed of mixing of the sample with $H_2^{18}O$ (175 $s^{-1}$ in the cited work), some doubts remained whether $W_f$ was indeed bound to the catalyst in the $S_2$ state. These were increased by the FTIR finding that one water molecule binds to the OEC during the $S_2 \rightarrow S_3$ transition [45,46]. Moreover, the mechanism derived by Siegbahn by DFT calculations [16,44] also suggests that the fast substrate–water is not, or only very weakly bound to the $Mn_4CaO_5$ cluster in the $S_2$ state.

The rate of fast substrate exchange, $k_f$, measured here for the $S_2$ state is very similar to that in the $S_3$ state, and therefore well resolved. If we exclude a diffusion limitation for the fast exchange in the $S_2$ state (NMRD experiments and theoretical calculations suggest much faster diffusion rates for water in proteins [47,48]), this finding demonstrates that in *C. merolae* PSII the fast water is bound in a similar way to the $Mn_4CaO_5$ cluster in the $S_2$ and $S_3$ states. Therefore, if a water binds during the $S_2 \rightarrow S_3$ transition, it cannot be the substrate during the present reaction cycle; it may rather be the 'next substrate', *i.e.* it will be oxidized during the next turnover of PSII [42,46].

### 4.2. Binding site for the fast exchanging substrate

The only 30 times faster exchange rate of $W_f$ compared to $W_s$ in the $S_2$ and $S_3$ states makes it rather unlikely that $W_f$ is bound to Ca. Not only because such a slow exchange of a terminal water ligand of Ca would be to our knowledge unprecedented [28,36], but also because the significant slowing of the rate of $W_f$ exchange — from the exchange rate being beyond resolution in the $S_1$ state to being rather similar to the rate of exchange of $W_s$ in the $S_2$ state — is hard to rationalize for a Ca-bound water. In contrast, binding to a Mn ion that is being oxidized from $Mn^{III}$ to $Mn^{IV}$ during the $S_1 \rightarrow S_2$ transition would provide a direct explanation for this finding.

Most recent DFT-based models of the catalytic cycle suggest that in the $S_2$ state the open cube structure is dominant and that in this configuration $Mn_{D1}$ is the last $Mn^{III}$ in the $S_2$ state, and that $Mn^{III}_{A4}$ is oxidized in the $S_1 \rightarrow S_2$ transition [16,49–51]. As such, $Mn_{A4}$ is the most likely binding site for $W_f$. Of the two waters bound in the crystal structure to $Mn_{A4}$ [6], only W2 is in a suitable position for O – O bond formation with O5. In addition, exchange experiments with ammonia have excluded W1 from being a substrate [30]. We therefore tentatively assign W2 to be the fast exchanging substrate $W_f$ [15,42].

### 4.3. Deceleration of the slow exchanging substrate in the $S_2 \rightarrow S_3$ transition

The third important information derived from this study is the deceleration of the slow water exchange in the $S_2 \rightarrow S_3$ transition. The slow exchange in the $S_3$ state of *C. merolae* PSII core particles is calculated to be 1.2 ± 0.3 $s^{-1}$ at 20 °C. This rate is ~2-fold slower than the slow rate previously determined for the $S_3$ state of spinach thylakoid membranes (2.2 ± 0.1 $s^{-1}$; 10 °C and 4.9 ± 0.3 $s^{-1}$; 20 °C) [23], but similar to those measured at 10 °C in core particles of spinach ($k_s$ = 1.1 $s^{-1}$) and *Thermosynechococcus elongatus* ($k_s$ = 0.5 $s^{-1}$), as well as *Synechocystis* PCC 6803 ($k_s$ = 0.9 $s^{-1}$) [25]. While in spinach the slow exchange rate was previously found to be identical in the $S_2$ and $S_3$ states, the $k_s$ rate determined here for the *C. merolae* PSIIcc clearly slows down during the $S_2 \rightarrow S_3$ transition. This deceleration can be caused by the structural change of the $Mn_4CaO_5$ catalyst that occurs upon the $S_2 \rightarrow S_3$ transition and/or by the additional oxidation of the OEC [13,52,53]. DFT calculations suggest that the exchange of Mn-bound water ligands is impossible in the $Mn^{IV}$ oxidation state. It was therefore proposed that water exchange in the $S_3$ state requires the equilibrium $S_3Y_Z \leftrightarrow S_2Y_Z^{\bullet}$ [36]. In such a situation an overall slowing of the exchange rates would be expected to occur during the $S_2 \rightarrow S_3$ transition, since the state in which water can exchange is available only for transient periods. As such, this exchange model would be qualitatively consistent with the present data, but in conflict with the exchange rates previously obtained for spinach samples. However, an alternative proposal involving the equilibrium between the above-

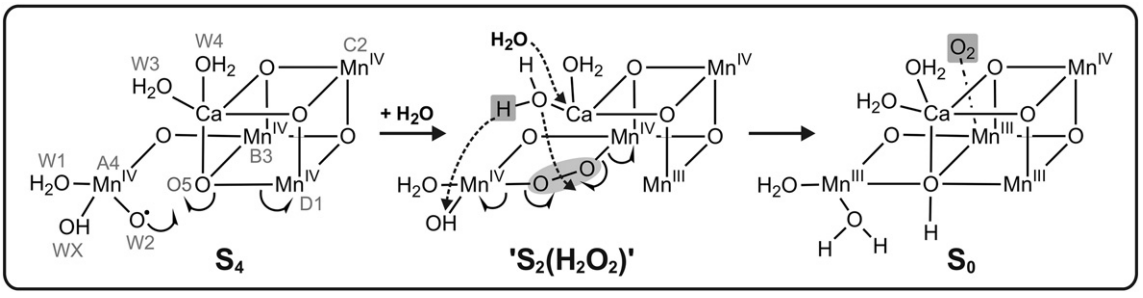


**Fig. 3.** Possible mechanism of $O_2$ formation during the $S_4 \rightarrow$ '$S_2(H_2O_2)$' $\rightarrow S_0$ transition. This suggestion [15,42,43,54] is based on the closed cube configuration of the $S_2$ state, and thus suggests that it is this configuration that proceeds to $S_3$ *via* water binding (WX) to $Mn_{A4}$.

described open and closed cube forms of the $Mn_4CaO_5$ cluster is also able to account for the present findings [42]. Species dependent changes may reflect a slight shift in the respective equilibria.

### 4.4. Implications for the mechanism of O – O bond formation

While more research is required to elucidate the mechanism of photosynthetic water oxidation, the strong binding of $W_f$ in the $S_2$ state described in this study provides further evidence for O – O bond formation between two Mn-bound substrates. The data thus favor direct coupling over nucleophilic attack mechanisms. Specifically, our present analysis points to W2 as being the fast exchanging substrate, $W_f$. Assuming that the $Mn_4CaO_5$ cluster attains in the $S_4$ state a structure that is similar to either the open or closed cube conformation reported for $S_2$ [38], the O – O bond could be formed with O5 being either in the outer, open cube position (geminal coupling) or, in our opinion more likely, it may couple with O5 while O5 is part of the distorted heteronuclear $CaMn_3O_4$ cube (closed cube) [15]. This latter option is presented schematically in Fig. 3.

## Acknowledgements

This work was supported by The Strong Research Environment Solar Fuels (Umeå University), the Artificial Leaf Project Umeå (K&A Wallenberg Foundation (grant KAW 2011.0055)), Energimyndigheten (grant 2012-005968-36648-1 to JM) and the Polish Ministry of Science and Higher Education/European Science Foundation (grant 844/N-ESFEuroSolarFuels/10/2011/0 to JK).

## References

[1] A. Zouni, H.T. Witt, J. Kern, P. Fromme, N. Krauß, W. Saenger, P. Orth, Crystal structure of photosystem II from *Synechococcus elongatus* at 3.8 Å resolution, Nature 409 (2001) 739–743.
[2] N. Kamiya, J.-R. Shen, Crystal structure of oxygen-evolving photosystem II from *Thermosynechococcus vulcanus* at 3.7 Å resolution, Proc. Natl. Acad. Sci. U. S. A. 100 (2003) 98–103.
[3] K.N. Ferreira, T.M. Iverson, K. Maghlaoui, J. Barber, S. Iwata, Architecture of the photosynthetic oxygen-evolving center, Science 303 (2004) 1831–1838.
[4] B. Loll, J. Kern, W. Saenger, A. Zouni, J. Biesiadka, Towards complete cofactor arrangement in the 3.0 Å resolution structure of photosystem II, Nature 438 (2005) 1040–1044.
[5] A. Guskov, J. Kern, A. Gabdulkhakov, M. Broser, A. Zouni, W. Saenger, Cyanobacterial photosystem II at 2.9 Å resolution and the role of quinones, lipids, channels and chloride, Nat. Struct. Biol. Mol. Biol. 16 (2009) 334–342.
[6] Y. Umena, K. Kawakami, J.-R. Shen, N. Kamiya, Crystal structure of oxygen-evolving photosystem II at a resolution of 1.9 Å, Nature 473 (2011) 55–60.
[7] P. Joliot, G. Barbieri, R. Chabaud, Un nouveau modele des centres photochimiques du systeme II, Photochem. Photobiol. 10 (1969) 309–329.
[8] B. Kok, B. Forbush, M. McGloin, Cooperation of charges in photosynthetic $O_2$ evolution, Photochem. Photobiol. 11 (1970) 457–476.
[9] J.P. McEvoy, G.W. Brudvig, Structure-based mechanism of photosynthetic water oxidation, Phys. Chem. Chem. Phys. 6 (2004) 4754–4763.
[10] E.M. Sproviero, J.A. Gascon, J.P. McEvoy, G.W. Brudvig, V.S. Batista, Quantum mechanics/molecular mechanics study of the catalytic cycle of water splitting in photosystem II, J. Am. Chem. Soc. 130 (2008) 3428–3442.
[11] G. Christou, J.B. Vincent, The molecular double-pivot mechanism for water oxidation, Biochim. Biophys. Acta 895 (1987) 259–274.
[12] W. Ruettinger, M. Yagi, K. Wolf, S. Bernasek, G.C. Dismukes, $O_2$ evolution from the manganese–oxo cubane core $Mn_4O_4^{6+}$: a molecular mimic of the photosynthetic water oxidation enzyme? J. Am. Chem. Soc. 122 (2000) 10353–10357.
[13] W. Hillier, T. Wydrzynski, The affinities for the two substrate water binding sites in the $O_2$ evolving complex of photosystem II vary independently during S-state turnover, Biochemistry 39 (2000) 4399–4405.
[14] V.K. Yachandra, The catalytic manganese cluster: organisation of the metal ions, in: T. Wydrzynski, K. Satoh (Eds.), Photosystem II. The Light-driven Water:Plastoquinone Oxidoreductase, Springer, Dordrecht, 2005, pp. 235–260.
[15] J. Messinger, Evaluation of different mechanistic proposals for water oxidation in photosynthesis on the basis of $Mn_4O_xCa$ structures for the catalytic site and spectroscopic data, Phys. Chem. Chem. Phys. 6 (2004) 4764–4771.
[16] P.E.M. Siegbahn, Water oxidation mechanism in photosystem II, including oxidations, proton release pathways, O – O bond formation and $O_2$ release, Biochim. Biophys. Acta 1827 (2013) 1003–1019.
[17] P. De Luca, R. Taddei, L. Varano, "Cyanidioschyzon merolae": a new alga of thermal acidic environments, Webbia 33 (1978) 37–44.
[18] M.J. Ferris, K.B. Sheehan, M. Kuhl, K. Cooksey, B. Wigglesworth-Cooksey, R. Harvey, J. M. Henson, Algal species and light microenvironment in a low-pH, geothermal microbial mat community, Appl. Environ. Microbiol. 71 (2005) 7164–7171.
[19] T.M. Bricker, J.L. Roose, R.D. Fagerlund, L.K. Frankel, J.J. Eaton-Rye, The extrinsic proteins of photosystem II, Biochim. Biophys. Acta 1817 (2012) 121–142.
[20] T. Krupnik, E. Kotabova, L.S. van Bezouwen, R. Mazur, M. Garstka, P.J. Nixon, J. Barber, R. Kana, E.J. Boekema, J. Kargul, A reaction center-dependent photoprotection mechanism in a highly robust photosystem II from an extremophilic red alga, *Cyanidioschyzon merolae*, J. Biol. Chem. 288 (2013) 23529–23542.
[21] A. Klauss, M. Haumann, H. Dau, Alternating electron and proton transfer steps in photosynthetic water oxidation, Proc. Natl. Acad. Sci. U. S. A. 109 (2012) 16035–16040.
[22] J. Messinger, M.R. Badger, T. Wydrzynski, Detection of *one* slowly exchanging substrate water molecule in the $S_3$ state of photosystem II, Proc. Natl. Acad. Sci. U. S. A. 92 (1995) 3209–3213.
[23] W. Hillier, J. Messinger, T. Wydrzynski, Kinetic determination of the fast exchanging substrate water molecule in the $S_3$ state of photosystem II, Biochemistry 37 (1998) 16908–16914.
[24] W. Hillier, J. Messinger, T. Wydrzynski, Substrate water $^{18}O$ exchange kinetics in the $S_2$ state of photosystem II, in: G. Garab (Ed.), Photosynthesis: Mechanisms and Effects, Kluwer Academic Publishers, Dordrecht, 1998, pp. 1307–1310.
[25] W. Hillier, G. Hendry, R.L. Burnap, T. Wydrzynski, Substrate water exchange in photosystem II depends on the peripheral proteins, J. Biol. Chem. 276 (2001) 46917–46924.
[26] W. Hillier, T. Wydrzynski, Substrate water interactions within the photosystem II oxygen evolving complex, Phys. Chem. Chem. Phys. 6 (2004) 4882–4889.
[27] G. Hendry, T. Wydrzynski, The two substrate water molecules are already bound to the oxygen evolving complex in the $S_2$ state of photosystem II, Biochemistry 41 (2002) 13328–13334.
[28] W. Hillier, T. Wydrzynski, $^{18}O$-water exchange in photosystem II: substrate binding and intermediates of the water splitting cycle, Coord. Chem. Rev. 252 (2008) 306–317.
[29] G. Hendry, T. Wydrzynski, $^{18}O$ isotope exchange measurements reveal that calcium is involved in the binding of one substrate–water molecule to the oxygen-evolving complex in photosystem II, Biochemistry 42 (2003) 6209–6217.
[30] M.P. Navarro, W.M. Ames, H. Nilsson, T. Lohmiller, D.A. Pantazis, L. Rapatskiy, M.M. Nowaczyk, F. Neese, A. Boussac, J. Messinger, W. Lubitz, N. Cox, Ammonia binding to the oxygen-evolving complex of photosystem II identifies the solvent-exchangeable oxygen bridge (μ-oxo) of the manganese tetramer, Proc. Natl. Acad. Sci. U. S. A. 110 (2013) 15561–15566.
[31] K.P. Bader, G. Renger, G.H. Schmid, A mass-spectrometric analysis of the water splitting reaction, Photosynth. Res. 38 (1993) 355–361.
[32] S. Isgandarova, G. Renger, J. Messinger, Functional differences of photosystem II from *Synechococcus elongatus* and spinach characterized by flash induced oxygen evolution patterns, Biochemistry 42 (2003) 8929–8938.
[33] N. Cox, D.A. Pantazis, F. Neese, W. Lubitz, Biological water oxidation, Acc. Chem. Res. 46 (2013) 1588–1596.
[34] H. Dau, I. Zaharieva, M. Haumann, Recent developments in research on water oxidation by photosystem II, Curr. Opin. Chem. Biol. 16 (2012) 3–10.
[35] K. Kawakami, Y. Umena, N. Kamiya, J.-R. Shen, Structure of the catalytic, inorganic core of oxygen-evolving photosystem II at 1.9 Å resolution, J. Photochem. Photobiol. B Biol. 104 (2011) 9–18.
[36] P.E.M. Siegbahn, Substrate water exchange for the oxygen evolving complex in PSII in the $S_1$, $S_2$, and $S_3$ states, J. Am. Chem. Soc. 135 (2013) 9442–9449.
[37] L. Rapatskiy, N. Cox, A. Savitsky, W.M. Ames, J. Sander, M.M. Nowaczyk, M. Rögner, A. Boussac, F. Neese, J. Messinger, W. Lubitz, Detection of the water-binding sites of the oxygen-evolving complex of photosystem II using W-band $^{17}O$ electron–electron double resonance-detected NMR spectroscopy, J. Am. Chem. Soc. 134 (2012) 16619–16634.
[38] D.A. Pantazis, W. Ames, N. Cox, W. Lubitz, F. Neese, Two interconvertible structures that explain the spectroscopic properties of the oxygen-evolving complex of photosystem II in the $S_2$ state, Angew. Chem. Int. Ed. 51 (2012) 9935–9940.
[39] D. Bovi, D. Narzi, L. Guidoni, The $S_2$ state of the oxygen-evolving complex of photosystem II explored by QM/MM dynamics: spin surfaces and metastable states suggest a reaction path towards the $S_3$ state, Angew. Chem. Int. Ed. 52 (2013) 11744–11749.
[40] H. Isobe, M. Shoji, S. Yamanaka, Y. Umena, K. Kawakami, N. Kamiya, J.R. Shen, K. Yamaguchi, Theoretical illumination of water-inserted structures of the $CaMn_4O_5$ cluster in the $S_2$ and $S_3$ states of oxygen-evolving complex of photosystem II: full geometry optimizations by B3LYP hybrid density functional, Dalton Trans. 41 (2012) 13727–13740.
[41] Y. Kurashige, G.K.-L. Chan, T. Yanai, Entangled quantum electronic wavefunctions of the $Mn_4CaO_5$ cluster in photosystem II, Nat. Chem. 5 (2013) 660–666.
[42] N. Cox, J. Messinger, Reflections on substrate water and dioxygen formation, Biochim. Biophys. Acta 1827 (2013) 1020–1030.
[43] P.E.M. Siegbahn, O – O bond formation in the $S_4$ state of the oxygen-evolving complex in photosystem II, Chem. Eur. J. 12 (2006) 9217–9227.
[44] P.E.M. Siegbahn, Structures and energetics for $O_2$ formation in photosystem II, Acc. Chem. Res. 42 (2009) 1871–1880.
[45] T. Noguchi, FTIR detection of water reactions in the oxygen-evolving centre of photosystem II, Philos. Trans. R. Soc. Lond. B 363 (2008) 1189–1194.
[46] H. Suzuki, M. Sugiura, T. Noguchi, Monitoring water reactions during the S-state cycle of the photosynthetic water-oxidizing center: detection of the DOD bending vibrations by means of Fourier transform infrared spectroscopy, Biochemistry 47 (2008) 11024–11030.
[47] S. Vassiliev, T. Zaraiskaya, D. Bruce, Molecular dynamics simulations reveal highly permeable oxygen exit channels shared with water uptake channels in photosystem II, Biochim. Biophys. Acta 1827 (2013) 1148–1155.
[48] E. Persson, B. Halle, Nanosecond to microsecond protein dynamics probed by magnetic relaxation dispersion of buried water molecules, J. Am. Chem. Soc. 130 (2008) 1774–1787.

[49] W. Ames, D.A. Pantazis, V. Krewald, N. Cox, J. Messinger, W. Lubitz, F. Neese, Theoretical evaluation of structural models of the $S_2$ state in the oxygen evolving complex of photosystem II: protonation states and magnetic interactions, J. Am. Chem. Soc. 133 (2011) 19743–19757.
[50] P.E.M. Siegbahn, Recent theoretical studies of water oxidation in photosystem II, J. Photochem. Photobiol. B Biol. 104 (2011) 94–99.
[51] S. Schinzel, J. Schraut, A.V. Arbuznikov, P.E.M. Siegbahn, M. Kaupp, Density functional calculations of $^{55}$Mn, $^{14}$N and $^{13}$C electron paramagnetic resonance parameters support an energetically feasible model system for the $S_2$ state of the oxygen-evolving complex of photosystem II, Chem. Eur. J. 16 (2010) 10424–10438.
[52] W. Liang, T.A. Roelofs, R.M. Cinco, A. Rompel, M.J. Latimer, W.O. Yu, K. Sauer, M.P. Klein, V.K. Yachandra, Structural change of the Mn cluster during the $S_2$ to $S_3$ state transition of the oxygen evolving complex of photosystem II. Does it reflect the onset of water/substrate oxidation? Determination by Mn X-ray absorption spectroscopy, J. Am. Chem. Soc. 122 (2000) 3399–3412.
[53] M. Haumann, C. Müller, P. Liebisch, L. Iuzzolino, J. Dittmer, M. Grabolle, T. Neisius, W. Meyer-Klaucke, H. Dau, Structural and oxidation state changes of the photosystem II manganese complex in four transitions of the water oxidation cycle ($S_0 \rightarrow S_1$, $S_1 \rightarrow S_2$, $S_2 \rightarrow S_3$, and $S_3$, $S_4 \rightarrow S_0$) characterized by X-ray absorption spectroscopy at 20 K and room temperature, Biochemistry 44 (2005) 1894–1908.
[54] D.J. Vinyard, G.M. Ananyev, G.C. Dismukes, Photosystem II: the reaction center of oxygenic photosynthesis, Annu. Rev. Biochem. 82 (2013) 577–606.